



# Detection of Pre-Skin Cancer Using Automatic Cell Segmentation Technique

Greeshma Rajan<sup>1</sup>

PG Scholar, Applied Electronics, SNS College of Engineering, Coimbatore, India<sup>1</sup>

**ABSTRACT:** Biopsy procedure needs invasive tissue removal from a living subject to determine the occurrence or extent of the diseases. It is complicated and time consuming processes. Third Harmonic Generated Microscopy is a new exemplar for non-invasive in vivo virtual biopsy which has the ability to obtain tissue images without removing tissues. The aim of this paper is to discuss about various virtual biopsy microscopic modalities and also about automatic cell segmentation approaches such as watershed transform and convergence index filter, which provides high accuracy for non-invasive analysis of cell Nuclear-to-cytoplasm ratio (NC ratio). NC ratio plays a vital role in identifying or detecting early disease symptoms such as skin cancers during medical imaging analysis.

**KEYWORDS:** Cell segmentation, Third Harmonic Generated Microscopy, Watershed transform, Convergence index filter, Nuclear-to-Cytoplasm (NC) ratio.

## I. INTRODUCTION

Detection of early skin cancer is done by a medical procedure named biopsy [2], which involves the removal of tissues from a living object. The removed tissue is processed by an extensive preparation procedure which includes fixing, embedding, sectioning, staining and placed under a microscope for pathologist examination. Errors may occur during tissue processing and it leads to in accurate diagnosis. It is painful, side effects may also occur like infection and spreading of cancer cells. Optical virtual biopsy techniques for cells and tissues imaging provides capable microscopic details about the benign and malignant lesions without tissue removal. This non-invasive in vivo virtual biopsy avoids or minimizes the above mentioned disadvantages involved in virtual biopsy procedure. It also reduces the cost and time consumption in traditional biopsy procedures.

Various non-invasive imaging techniques such as con-focal microscopy [2], two-photon fluorescence (2PF) microscopy, and second harmonic generation (SHG) microscopy have been developed and applied for in vivo human skin diagnosis. Skin disease changes may occur in the deep dermis layer of the skin i.e., several hundred microns below the skin surface. Above mentioned techniques are limited by photo damage, lower resolution, lower penetrability or low contrast. Higher harmonic generation microscopy (HHG) [1], which combines the second and third harmonic generation modalities based on 1230-1250 nm, and can provide high penetration, high resolution and rich contrast. Second harmonic generation (SHG) light nearly disappeared beyond the depth of 200 $\mu$ m, and the image produced by the SHG also becomes out of focus and lose sharpness at a depth of 250  $\mu$ m, but still visible at a range of 350 $\mu$ m. THG gives a clear boundary definition between the cell nuclei and cytoplasm [1]. Nuclear-to-Cytoplasm [1] ratio plays a vital role in identifying early symptoms of diseases like skin cancer, whose ratio is generally larger in skin cancer than in normal cells and also, provides information about the type and stage of the disease. Several cell segmentation algorithms have been established for describing the exact position of the round objects and gives information about the size, shape and area to obtain useful properties. Image thresholding [4]-[6] is one of the cell segmentation methods used to segment the objects out of background; it lacks adaptability for global thresholding. This method is computationally expensive and does not consider clustered cells i.e., it cannot separate the touching nuclei. Watershed based-segmentation [4], is a popular morphological image segmentation tool, and often produces over segmentation due to false markers. To reduce over-segmentation fragment merging [6] and marker-controlled watershed transform are used. Fragment merging [6], combines the compactness score and probability density function (PDF) score to obtain more



correctly segmented nuclei but, it is sensitive to the size of nuclei. Marker-controlled watershed [7]-[8], replaces the region minimum with predefined markers, each of which represents the object but, the difficulty in performing this method is marker extraction. Convergence index filter [9]-[10], degree of convergence is based on the distribution of the gradient vector not on their magnitude. It is based on the maximization of the convergence index at each point of the spatial co-ordinates. Some of the convergence index filters are COIN filter, Adaptive Ring filter, IRIS filter, Sliding Band filter (SBF). Support region, is the major difference among these filters. In this paper [1], we discuss about how marker-controlled watershed transform combines with sliding band convergence index filter works for the automatic cell segmentation in vivo virtual biopsy images of human skin.

## II. IMAGE ACQUISITION BACKGROUNDS

Almost all the parts of our body is completely covered by skin, to precisely diagnose the skin diseases, biopsy is the most common method used today. But, it is invasive, painful to the patient and may also risk patient's life by causing infection or spreading of cancer cells. And, it consumes time for fixing, embedding and staining or pathological analysis. For early diagnosis of skin diseases invasive physical biopsy procedures are removed by non-invasive in vivo virtual biopsy. Confocal microscopy [2], Two photon fluorescence (2PF) microscopy, Second Harmonic Generation (SHG) microscopy, Higher Harmonic Generation (HHG) microscopy, which combines the second and third harmonic generation (THG) microscopy are some of the non-invasive in vivo virtual biopsy imaging techniques.

### THIRD HARMONIC GENERATION MICROSCOPY

Gwo Giun et al. (2013) proposed an automatic cell segmentation [1] approach for analysing nuclear-to-cytoplasm(NC) ratio for third-harmonic generated virtual biopsy images. Third-Harmonic Generation (THG) [1] is a nonlinear process, related to the interaction of light with matter, which generates light waves with three times the frequency of the source. It obeys the laws of conservation of energy and involves virtual electron transitions alone. Hence, there is a possibility of less photo damage and photo bleaching and no energy deposition on the interacted matters. THG [3] signals measured on the chicken skin, muscle and fat and stronger THG signals have been found in the skin. Based on that, THG microscopy applied in wide areas, such as the microscopic imaging of plant leaf cells, cultured cells, live zebra-fish embryos and lives mouse skin. THG arises from cell membrane, cytoplasm organelles, hemoglobin, elastic fiber and lipid bodies and it is mainly subscribe by the cytoplasm of the keratinocytes, boundaries of collagen fibers and red blood cells where SHG provides the collagen fibers in the dermis. The resolution of each image is 512 x 512 and is stored in gray-level 12-bit TIFF files, where pixel values are proportional to their third harmonic responses. Fig. 3(a) shows an image from our dataset in which equal amounts of third harmonic responses have been provided in red and blue channels for visualization purposes. The magenta region represents cytoplasm, and the dark part surrounded by magenta cytoplasm represents nuclei. The proposed algorithm for cell segmentation is not limited to these images but can be utilized for analysis of other multivariate images.

## III. CELL SEGMENTATION TECHNIQUES

The block diagram of cell segmentation and NC ratio analysis(Fig. 1) is divided into two parts: nuclei and cytoplasm segmentation. We use gradient watershed transform [13]-[16] based on the contextual information of pixels in images for nuclei segmentation. The main objective of watershed transform is to identify regional minima in original images, which are usually the regions of nuclei to be segmented. First, we calculate the gradient map to highlight the nuclei boundary. The homogeneous regions in the gradient map correspond to the regional minima in the input image. We refrain from performing nuclei detection directly on the gradient map because its incidental regional minima or noise would cause over-segmentation. Instead, nuclei initialization with marker-controlled strategy and detection must be performed at the beginning of nuclei detection.

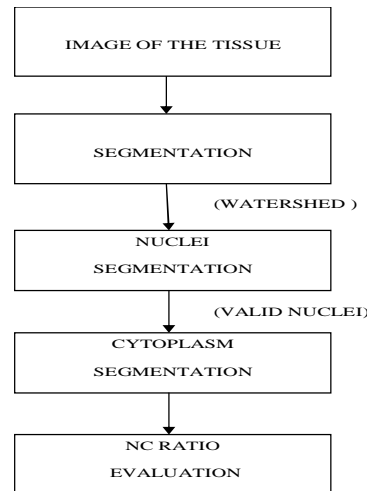


Fig. 1. Block diagram of cell segmentation and NC ratio analysis.

For nuclei initialization, potential nuclei and their corresponding cell boundaries can be obtained to help design a filter to remove the incidental regional minima from the gradient map. The filtered gradient map would then be subject to nuclei detection using watershed transform, yielding segmented nuclei. Nuclei validation must also be considered, using a shape descriptor to exclude the outliers and preserve the valid nuclei. Of course, if we have user interaction or some prior information in the analysis procedure, the results will be convincing for medical diagnosis. For cytoplasm segmentation, cytoplasm initialization would be performed based on the information of valid nuclei to obtain potential cytoplasms and corresponding refined cell boundaries. Then, a local filter is designed to be used in the cytoplasm detection stage to obtain segmented cytoplasm. Finally, the evaluated NC ratios are obtained in the NC ratio evaluation stage.

#### A. Nuclei Segmentation

Nuclei segmentation is performed using gradient watershed transform with marker-controlled strategy, blob detection, and consideration of shape descriptors to obtain accurate segmented nuclei. Nuclei segmentation is a crucial stage in the proposed cell segmentation algorithm because the subsequent stage of cytoplasm segmentation references valid nuclei, which can be thought of as the initial condition of the optimization problem of whole cell segmentation in order to guide the algorithm in finding a feasible solution with high performance.

##### 1) Watershed Transform With Marker-Controlled Strategy:

Watershed transform [13]–[16], which considers contextual information in an image and identifies the regional minima, is chosen here for nuclei segmentation. In observation of images, nuclei with lower intensity locate in the regional minima of images, which are highly correlated with homogeneous regions in the gradient map. Therefore, we utilize the gradient map with prior information for the boundaries of nuclei to help to extract and analyze the almost uniform and round nuclei of adjacent cells from the background. To have a robust gradient map, we use the Sobel operator and Roberts's cross-gradient operator [12] to calculate gradient maps in the horizontal, vertical, and positively sloped diagonal, and negatively sloped diagonal directions. If nuclei detection is performed using direct watershed transform of the gradient map, it may suffer from the problem of over-segmentation due to the existence of undesired regional minima and irrelevant noise in the gradient map. So we should design a filter that should be implemented at the initial stage of nuclei detection to exclude the undesired regional minima and preserve the desired ones.

Nuclei initialization would prevent over-segmentation by adopting the marker-controlled strategy followed by the technique of minima imposition existing in morphological image processing. Two kinds of markers are needed: those that roughly mark the locations of potential nuclei and those that mark their corresponding cell boundaries. These two kinds of markers are defined respectively as

- Internal markers: the groups of connected pixels inside each region where the potential nucleus is to be segmented.
- External markers: the groups of connected pixels ideally relative to the boundary of each cell.

The internal markers are the initial points that guide the watershed transform to obtain the desired solution that fits the size and shape of the desired nuclei while external markers prevent over-flooding in the watershed transform.

## 2) Nuclei Initialization:

The objective of nuclei initialization is to obtain the potential nuclei and their corresponding cell boundary using blob detection followed by outlier removal as well as distance transform. The main block diagram of nuclei initialization is presented in Fig. 2. The potential nuclei are marked with internal markers, and the corresponding cell boundaries are marked with external markers. Internal markers must meet the following criteria:

- Regions of internal markers must be surrounded by pixels of higher intensity.
- All pixels in each region of internal markers should form a connected component with homogeneous intensity.

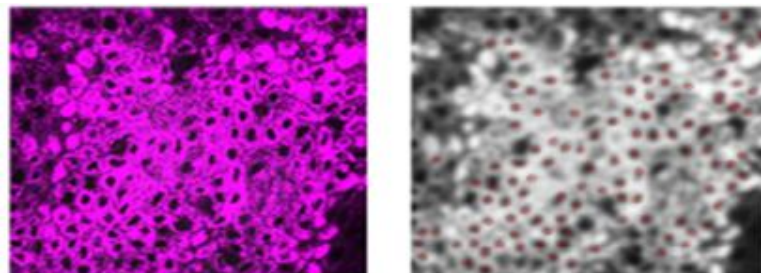
To determine the internal markers, blob detection is performed with prior information of the nuclei to be segmented. Outliers of nuclei candidates are excluded by outlier removal to obtain potential nuclei, which are also called internal markers. Subsequently, distance transform of internal markers is performed to obtain a distance map followed by cell boundary initialization to determine the potential cell boundaries, which are also called external markers. Of course, user interaction can also be considered for marker determination in nuclei initialization when medical doctors or staff expects to analyze the specific cells of interest.

### a) Blob detection

For blob detection, the original image to be segmented is spanned into the scale-space to interpret the multi-scale representation of the image in order to extract structures of interest or feature points with the scale and spatial information concurrently. Then the input image into the scale-space with Gaussian kernel utilized the scale-space derivatives to extract the scale and spatial information of blobs concurrently in the images. The scale-space representation of a two-dimensional image is denoted by

$$L(.;.;\sigma) = f(.;.) * g(.;.;\sigma) \quad (1)$$

Where  $g$  is the Gaussian operator denoted by  $g(x,y;\sigma) = (1/2\pi\sigma^2)e^{-(x^2+y^2)/2\sigma^2}$  where  $\sigma$  is the scale parameter, and \* represents the convolution operator. To extract the appropriate scale and locality information simultaneously, scale-space derivatives and a Hessian matrix are adopted for local extrema detection to obtained blob information. The objective of nuclei initialization is to obtained the potential nuclei and their corresponding cell boundary using blob detection. For blob detection, the original image to be segmented is spanned into the scale-space to interpret the multi-scale representation of the image in order to extracted structures of interest or feature points with the scale and spatial information, which is as shown in figure2.



(a) Input image

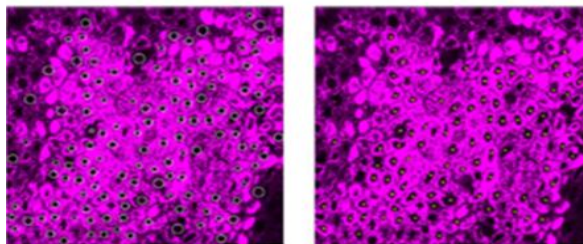
(b) Detected blobs on the scale-space representation

Figure.2 Simulation result of blob detection

From the Figure.2(a), the input image of the tissue and its scale-space representation are observed. Different actual sizes of blobs are distinguished on the scale-space representation at different scales. The detected blob maps at scale with red circles are obtained in Figure.2(b).

#### b) Outlier

Removed the possible outliers as among the nuclei candidates required applying local constraints. The valid nuclei must be surrounded by cytoplasm that has sufficient intensity and area. Nuclei candidates in an original image with existing outliers and some candidates are not surrounded completely by cytoplasm. The nuclei candidates without outliers that are considered as potential nuclei are called as internal markers. Local constraints adaptive to blob size are considered to exclude the outliers and preserve the valid nuclei that are completely surrounded by cytoplasm having sufficient intensity and area which has been presented in Figure5.2.



(a) Nuclei candidates with existing outliers. (b) Potential nuclei without outliers (Internal marker)

Figure3. Simulation result of outlier

From the Figure3.(a), it has been observed that the nuclei candidates in an original image with existed outliers and some candidates that are not surrounded completely by cytoplasm. Figure.2 (b) presented the nuclei candidates without outliers, which are considered as potential nuclei and called internal markers.

#### c) Distance transforms

The detected blobs without outliers serve as the internal markers marking the rough position of potential nuclei. External markers roughly delineating cell boundaries will help of the complete marker map for the watershed transform with the marker-controlled strategy. Since the external markers must not be too close to the boundaries of the regions that are nuclei to be segmented, then calculated the Euclidean distance maps of the internal-marker map, which comprise the Euclidean distance between each pixel and the nearest pixel belonging to an internal marker. The Euclidean distance map represented the original binary image by labeled each pixel with the Euclidean distance between that pixel and the nearest non-zero pixel in a binary image, which generated a useful representation in the area of cell segmentation. The internal-marker map roughly demarcated the potential nuclei, and the external-marker map roughly draws the cell boundary. In addition, the external markers partitioned the image into many regions, each of which contains only one internal marker. This has simplified the problem of cell segmentation by partitioning each of these regions into two parts: a single object that could be only one pixel or a connected component inside the nucleus to be segmented and its background. This brings about one-to-one correspondence between the markers and the segmentation result, which can enhance the accuracy of nuclei segmentation.

#### 3) Morphological Image Processing

The internal and external marker map marked the potential nuclei and their corresponding cell boundaries, respectively, which are required for the watershed transform with a marker-controlled strategy, and designed a filter using morphological minima imposition to removed the undesired regional minima in the gradient map and preserve the desired ones to resolved the over-segmentation problem of the watershed transform. The minima imposition is one of the techniques in morphological image processing to limit the regional minima to the location of pixels belonging to marker map. Then the internal and external markers are used to perform minima imposition on the gradient map to

obtained a filtered gradient map whose regional minima only occur at the location of internal and external marker pixels.

#### 4) Nuclei Detection and Validation

The watershed transform is used again to calculate the watersheds of the filtered gradient map and obtained the segmented nuclei from original skin cell images. To ensure that the nuclei have been accurately segmented, also considered their shape. Shape descriptors are the crucial measures in the applications of computer vision and pattern recognition, and especially in microscopy imaging analysis, where they help exclude undesired objects. Compactness which indicates irregularity associated with cancer cells, is utilized in this stage of nuclei validation and is defined as

$$\text{Compactness} = A/P^2 \quad (2)$$

Where A - area of the object, P - perimeter of the object. From the observations of THG images, the shape of cells is very closed to circular or elliptical with higher compactness. Using this property to exclude undesired objects having low compactness. The segmented nuclei without consideration of shape compactness in which that do not belong to nuclei. Valid nuclei considered shape compactness in which confident nuclei are preserved with higher compactness and outliers with lower compactness have been removed to enhance the accuracy of segmentation results. White valid nuclei are also imposed on the original image for visualization; the accuracy of nuclei segmentation thus produced is desirable. If nuclei detection is performed using direct watershed transform of the gradient map, it must suffer from the problem of over-segmentation due to the existence of undesired regional minima and irrelevant noise in the gradient map. So design a filter that should be implemented at the initial stage of nuclei detection to exclude the undesired regional minima and preserve the desired ones. The watershed transform is used to calculate the watersheds of the filtered gradient map and obtained the segmented nuclei is presented in Figure 2. From original skin cell images. White valid nuclei are also imposed on the original image as presented for visualization; the accuracy of nuclei segmentation thus produced is desirable. From the Figure 4.(a), it can be observed that the segmented nuclei without consideration of shape compactness, in which exist several outliers with lower compactness that does not belong to nuclei. From the Figure 4.(b), it can be observed the valid nuclei considered the shape compactness in which confident nuclei are preserved with higher compactness and outliers with lower compactness has been removed to enhance the accuracy of segmentation results.



a) Without consideration of shape compactness. (b) With consideration of shape compactness.

Figure 4. Simulation result of segmented nuclei

#### B) CYTOPLASM SEGMENTATION

For cytoplasm segmentation, a convergence index filter with parameter setting is adopted based on valid nuclei. It is considered as gradient vectors instead of intensity of images, a convergence index filter is suitable for low-contrast and noisy microscopy images. Such a filter made unnecessary the pre-processing to enhance contrast and removed irregular noise in biomedical images, which will preserve the information needed for clinical diagnosis. The parameter setting for convergence index filter is used to adjust easily without technical details of algorithmic processing according to

some fundamental information of input biomedical images to be analyzed like size or shape of cells. But the convergence index filters considered the contextual and locality information to have confident segmentation results and reduced the uncertainty of segmentation resulting from low contrast and noise in images. Several assumptions should be made for using convergence index filtering to segment the cytoplasm:

- The shape of cells and their corresponding nuclei are all convex regions.
- Each cytoplasm and its corresponding nucleus are almost concentric, and the gradient vector of each pixel belonging to the cytoplasm and its corresponding nucleus has a trend to point toward the same cell center.

### 1) Cytoplasm initialization

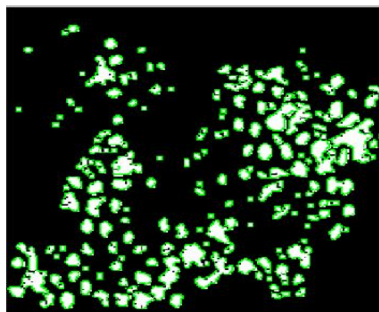
First, to determined two constraints,  $R_{\min}$  and  $R_{\max}$  which represented the minimum distance the inner boundary and the maximum distance from the outer boundary to the center P of the support region on each orientation, respectively. These two constraints are adaptive to the shape and position of each valid nucleus. The boundary of each valid nucleus can be thought of as a minimum boundary  $R_{\min}$  of cytoplasm on that cell that makes sure that the candidates of cytoplasmic region are not presented in the nuclear region. For determined the  $R_{\max}$ , then used the concept of distance transform to generate the refined distance map of to delineated the maximum boundary of potential cytoplasmic region for each cell. Therefore, the robust and confident restriction of boundary of potential cytoplasmic region with adaptive constraints  $R_{\min}$  and  $R_{\max}$ , for each cell, which can not only avoid overlap of segmented cells but also resolve issues of cell segmentation of adjacent cells with indistinct boundaries in multivariate biomedical images.

### 3) Cytoplasm Detection

After finding the  $R_{\min}$  and  $R_{\max}$ , for each cell, the support region of the proposed local filter can be thought of as the union of N line segments  $Q_j Q_j^1$ , which represented the cytoplasmic width radiating from cell center P on each orientation. Here, the definition of the convergence index of the gradient vector is almost the same as that of the sliding band filter, but some constraints about variable distance between cell center and the outer boundary of the supported region on each orientation are different. The output of the local filter applied to the pixel of interest of Cartesian coordinate (x,y) is defined as the average of convergence indices on line segments  $Q_j Q_j^1$  in 2-D discrete space

$$Filter(x, y) = \frac{1}{N} \sum_{j=0}^{N-1} F_j(x, y) \quad (3)$$

where N is the number of half-lines radiating from the pixel of interest P,  $Filter(x, y)$  is the average of the convergence indices on the  $j^{th}$  line segments  $Q_j Q_j^1$ ,  $R_{\min}$  and  $R_{\max}$  are the minimum and maximum distance from the pixel of interest to inner and outer boundary on the  $j^{th}$  half-line respectively. Using the above valid nuclei the cytoplasm is segmented. The valid nuclei must be surrounded by cytoplasm that has sufficient intensity and area, which has been presented in Figure.5



(a) Segmented cytoplasm

Figure .5 Simulation result of cytoplasm segmentation



2.5 CELL SIZE AND NC RATIO EVALUATION

Cellular size and nuclear size are indicators not only of the developing status of some diseases but of skin and other quantifiable physical factors. For example, cellular and nuclear size in the layers of basale cells in forearm skin has been found to increase with age. The NC ratio, which has been defined as the volume ratio of nucleus to cytoplasm, is commonly used in diagnosis. A protocol has been developed to obtain accurate NC ratios. Although the NC ratio is defined as a volume ratio, it can be approximated by an area ratio of nucleus to cytoplasm.

IV. EXPERIMENTAL RESULTS

Automatic cell segmentation and NC ratio evaluation were performed using the proposed algorithm on about 600 THG virtual biopsy images of the stratum basale layer of human forearm skin from 31 healthy volunteers. The evaluated NC ratios and cell sizes were discussed and interpreted by a dermatologist and a radiologist. From the Figure 5.4(a), it can be observed that one of the experimental results of cell segmentation is given. Its profile, including the evaluated NC ratios, cell sizes, and position is given in Table 5.1. Most of the cells were segmented accurately. Moreover, user interaction with medical doctors or medical staff can be adopted to exclude mistakenly segmented cells further with the profiles that recorded the information of each segmented cell or selected the specific cells of interest to enhance the performance of cell segmentation and NC ratio evaluation in clinical diagnosis.

Cell Index	Cell Area (pixels)	Nuclear Area (pixels)	Cytoplasmic Area(pixels)	NC Ratio
1	924	229	695	0.329496403
2	649	160	489	0.327198364
3	901	228	673	0.338781575
4	1076	316	760	0.415789474
5	836	201	635	0.316535433
....	....			
149	862	222	640	0.326875
150	972	319	653	0.488514548
151	943	296	647	0.4574970297
152	722	217	505	0.32970297
153	1226	303	923	0.328277356
154	1221	408	813	0.501845018
155	1357	400	957	0.417972832
156	1341	452	889	0.508436445
157	1323	195	1128	0.28672234
158	1066	265	801	0.330836454
Total	56250	15732	40518	-
Average	969.8276 (pixels)	271.2414 (pixels)	698.5862 (pixels)	0.325971879

Table 5.1 Calculation of NC Ratio

From the table 5.1 it can be observed that the experimental results of cell segmentation including the evaluated NC ratios, cell sizes and also found that the range of NC ratio lies between 0.29-0.51 with average 0.326.





## V. CONCLUSION

This method presented a computer-aided design for automatic cell segmentation and NC ratio analysis. Realization of automatic cell segmentation has been studied using a watershed algorithm. Here the nuclei and cytoplasm are segmented from tissue image and then found the NC ratio from it. A MATLAB programming has been developed for the implementation of this method. NC ratio value is achieved by this proposed method is 0.29-0.51 and mean and standard deviation are 0.33, 0.01 respectively. The proposed method saves much time and provides convincing segmentation result. Processing time can be reduced by using this technique.

## REFERENCES

- [1] Gwo Giun (Chris) Lee, Senior Member, IEEE, Huan-Hsiang Lin, Ming-Rung Tsai, Sin-Yo Chou, Wen-Jeng Lee, Yi-Hua Liao, Chi-Kuang Sun, Fellow, IEEE, and Chun-Fu Chen, 'Automatic Cell Segmentation and Nuclear-to-Cytoplasmic Ratio Analysis for Third Harmonic Generated Microscopy Medical Images', IEEE Transactions On Biomedical Circuits And Systems, Vol. 7, pp. 158-168, 2013.
- [2] S.-Y. Chen, H.-Y. Wu and C.-K. Sun, 'In vivo harmonic generation biopsy of human skin', J. Biomed. Opt., vol. 14, no. 6, p. 060505, 2009.
- [3] S.-Y. Chen, S.-U. Chen, H.-Y. Wu, W.-J. Lee, Y.-H. Liao and C.-K. Sun, 'In vivo virtual biopsy of human skin by using non invasive higher harmonic generation microscopy', IEEE J. Sel. Topics Quantum Electron., vol. 16, no. 3, pp. 478-492, 2010.
- [4] K. Z. Mao, Peng Zhao, and Puay-Hoon Tan, 'Supervised Learning-Based Cell Image Segmentation for P53 Immuno histo chemistry', IEEE Transactions On Biomedical Engineering, Vol. 53, pp. 1153-1163, 2006.
- [5] Bin Fang, Wynne Hsu, and Mong Li Lee, 'On the Accurate Counting of Tumor Cells', IEEE Transactions On Nanobioscience, Vol. 2, pp.94-103,2003.
- [6] Xiaobo Zhou, Fuhai Li, Jun Yan, and Stephen T. C. Wong, 'A Novel Cell Segmentation Method and Cell Phase Identification Using Markov Model', IEEE Transactions On Information Technology In Biomedicine, Vol. 13, pp.152-157, 2009.
- [7] Chanho Jung and Changick Kim, 'Segmenting Clustered Nuclei Using H-minima Transform-Based Marker Extraction and Contour Parameterization', IEEE Transactions On Biomedical Engineering, Vol. 57, pp.2600-2604, 2010.
- [8] Xiaodong Yang, Houqiang Li, and Xiaobo Zhou, 'Nuclei Segmentation Using Marker-Controlled Watershed, Tracking Using Mean-Shift, and Kalman Filter in Time-Lapse Microscopy', IEEE Transactions On Circuits And Systems Vol. 53, pp. 2405-2414, 2006.
- [9] Hidefumi Kobatake, and Shigeru Hashimoto, 'Convergence Index Filter for Vector Fields', IEEE Transactions On Image Processing, Vol. 8, pp.1029-1038, 1999.
- [10] Pedro Quelhas, Monica Marcuzzo, Ana Maria Mendonça and Aurélio Campilho, 'Cell Nuclei and Cytoplasm Joint Segmentation Using the Sliding Band Filter', IEEE Transactions On Medical Imaging, Vol. 29, pp. 1463-1473, 2010.
- [11] Hyejun Ra, Wibool Piyawattanametha, Yoshihiro Taguchi, Daesung Lee, Michael J. Mandella, 'Two-Dimensional MEMS Scanner for Dual-Axes confocal Microscopy', Journal of microelectromechanical systems, Vol. 16, No.4, 2007.
- [12] Kung-Bin Sung, Chen Liang, Michael Descour, Tom Collier, Michele Follen, and Rebecca Richards-Kortum, 'Fiber-Optic Confocal Reflectance Microscope With Miniature Objective for In Vivo Imaging of human skin tissues', IEEE Transaction on Biomedical Engineering, Vol. 49, pp. 1168-1172, 2002.
- [13] Terry B. Huff, Yunzhou Shi, Yan Fu, Haifeng Wang and Ji-Xin Cheng, 'Multi-modal Nonlinear Optical Microscopy and Applications to Central Nervous System Imaging', IEEE journal on Quantum Electronics, Vol. 14, pp.4-9, 2008.
- [14] Paul J. Campagnola, Heather A.Clark, William A. Mohler, Aaron Lewis, Leslie M. Loew, 'Second-harmonic imaging microscopy of living cells', Journal of Biomedical Optics, 2001.